

ColPali: Efficient Document Retrieval with Vision Language Models

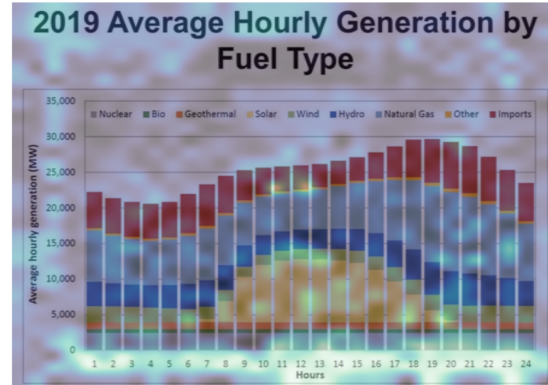
Manuel Faysse^{*1,3} Hugues Sibille^{*1,4} Tony Wu^{*1}
Gautier Viaud¹ Céline Hudelot³ Pierre Colombo^{2,3}
¹Illuin Technology ²Equall.ai
³CentraleSupélec, Paris-Saclay ⁴ETH Zürich
manuel.faysse@centralesupelec.fr

Abstract

Documents are visually rich structures that convey information through text, as well as tables, figures, page layouts, or fonts. While modern document retrieval systems exhibit strong performance on query-to-text matching, they struggle to exploit visual cues efficiently, hindering their performance on practical document retrieval applications such as Retrieval Augmented Generation. To benchmark current systems on visually rich document retrieval, we introduce the Visual Document Retrieval Benchmark *ViDoRe*, composed of various page-level retrieving tasks spanning multiple domains, languages, and settings. The inherent shortcomings of modern systems motivate the introduction of a new retrieval model architecture, *ColPali*, which leverages the document understanding capabilities of recent Vision Language Models to produce high-quality contextualized embeddings solely from images of document pages. Combined with a late interaction matching mechanism, *ColPali* largely outperforms modern document retrieval pipelines while being drastically faster and end-to-end trainable. We release all project artifacts at <https://huggingface.co/vidore>.

1 Introduction

Document Retrieval consists in matching a user query to relevant documents in a given corpus. It is central to many industrial applications, either as a standalone ranking system (search engines) or as part of more complex information extraction or Retrieval Augmented Generation (RAG) pipelines. Over recent years, pretrained language models have enabled large improvements in text embedding models. In practical industrial settings, however, the main performance bottleneck for efficient document retrieval is not in embedding model performance but in the prior data ingestion pipeline. To index a standard PDF document, many steps are



Query: "Which hour of the day had the highest overall electricity generation in 2019?"

Figure 1: For each term in a user query, **ColPali** identifies the most relevant document image patches (highlighted zones) and computes a query-to-page matching score. We can then swiftly retrieve the most relevant documents from a large pre-indexed corpus.

required. First, PDF parsers or Optical Character Recognition (OCR) systems are used to extract words from the pages. Document layout detection models can then be run to segment paragraphs, titles, and other page objects such as tables, figures, and headers. A chunking strategy is then defined to group text passages with some semantical coherence, and modern retrieval setups may even integrate a captioning step to describe visually rich elements in a natural language form, more suitable for embedding models. In our experiments (Table 2), we typically find that optimizing the ingestion pipeline yields much greater performance on visually rich document retrieval than optimizing the text embedding model.

Contribution 1: *ViDoRe*. In this work, we argue that document retrieval systems should not be evaluated solely on the capabilities of text embedding models (Bajaj et al., 2016; Thakur et al., 2021; Muennighoff et al., 2022), but should also consider the context and visual elements of the doc-

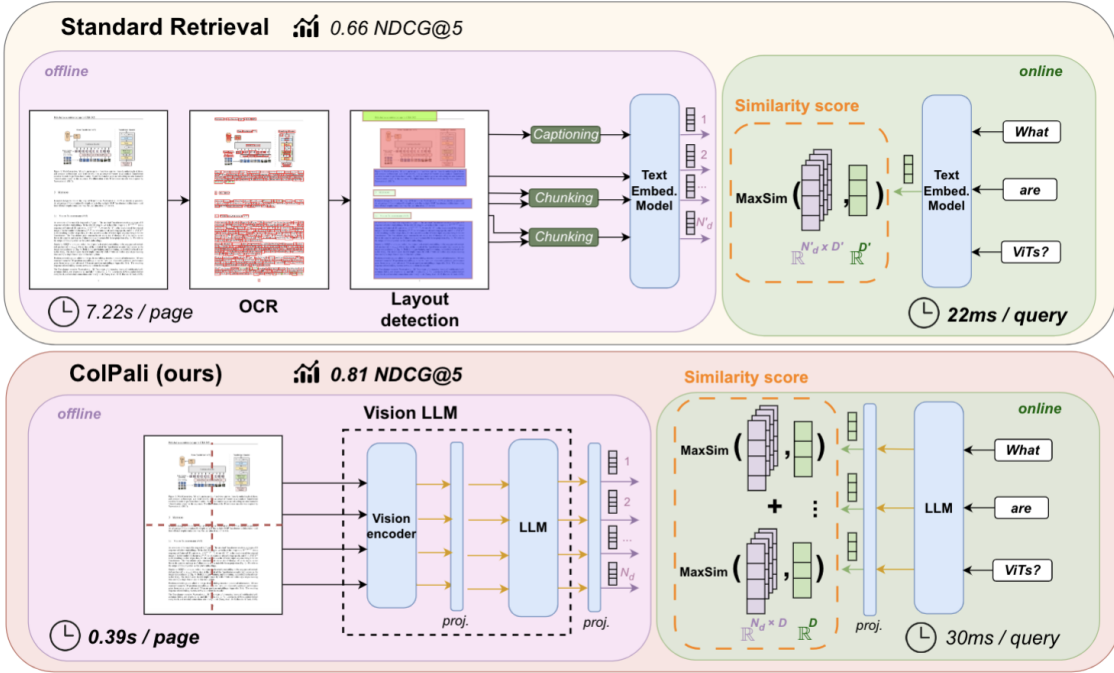


Figure 2: *ColPali* simplifies document retrieval w.r.t. standard retrieval methods while achieving stronger performances with better latencies. Latencies and results are detailed in section 5 and subsection B.5.

uments to be retrieved. To this end, we create and openly release *ViDoRe*, a comprehensive benchmark to evaluate systems on page-level document retrieval with a wide coverage of domains, visual elements, and languages. *ViDoRe* targets practical document retrieval settings, in which user queries may require both textual and visual understanding to be correctly matched to relevant documents. We highlight the shortcomings of current text-centric systems in these settings.¹

Contribution 2: *ColPali*. We propose a novel model architecture and training strategy based on Vision Language Models (VLMs) to efficiently index documents purely from their visual features, allowing for subsequent fast query matching with late interaction mechanisms (Khattab and Zaharia, 2020). Our method, *ColPali*, outperforms all other retrieval systems on *ViDoRe* while being fast and end-to-end trainable. We release models and code at <https://huggingface.co/vidore>.

2 Problem Formulation & Related Work

Problem Setting. In our setting, a retrieval system scores how relevant a document d from corpus \mathcal{D} is with respect to a query q . Computing the similarity

¹The benchmark leaderboard is hosted publicly at <https://huggingface.co/spaces/vidore/vidore-leaderboard> to encourage further developments.

score $s(q, d) \in \mathbb{R}_+$ for each of the $|\mathcal{D}|$ documents in the corpus creates a ranking we can use to extract the most relevant documents. In this work, we focus on page-level retrieval: *given a query, is the correct document page retrieved by the system?* For coherence with existing literature, we further use the term *document* to refer to individual pages, i.e. the atomic retrieved elements in our setting. As we focus on practical industrial retrieval applications (RAG, search engines) with potentially large corpora sizes, latency constraints are imposed on scoring systems. Most current retrieval systems can be decomposed into (1) an *offline* indexation phase in which a document index is built and (2) an *online* querying phase in which a query is matched to documents from the index and where low latency is vital to the user experience.

Efficient document retrieval systems exhibit joint properties of high retrieval performance (R1), low latency during querying (R2), and high throughput during indexation (R3).

2.1 Textual Retrieval Methods

Document Retrieval in Text Space. Statistical methods based on word frequency like TF-IDF (Sparck Jones, 1972) and BM25 (Robertson et al., 1994) are still widely used due to their simplicity and efficiency. More recently, neural embedding

models based on fine-tuned large language models display state-of-the-art performance on a variety of text embedding tasks and top the retrieval leaderboards (Muennighoff et al., 2022).

Neural Retrievers. In bi-encoder models (Reimers and Gurevych, 2019; Karpukhin et al., 2020; Wang et al., 2022), documents are independently mapped *offline* to a dense vector space. Queries are embedded *online* and matched to documents through a fast cosine distance computation. A slower, but slightly more performant alternative, cross-encoder systems (Wang et al., 2020; Cohere, 2024) concatenate query and document as a single input sequence and iteratively attribute matching scores to each possible combination. This enables full attention computation between query and document terms but comes at the cost of computational efficiency, as $|\mathcal{D}|$ encoding passes must be done online.

Multi-Vector retrieval via late interaction. In the late interaction paradigm (Khattab and Zaharia, 2020), an embedding is pre-computed and indexed per document token. At runtime, similarity can be computed with individual query token embeddings. The idea is to benefit from the rich interaction between individual query and document terms while taking advantage of the offline computation and fast query matching enabled by bi-encoders.

Retrieval Evaluation. Although benchmarks and leaderboards have been developed to evaluate text embedding models (Thakur et al., 2021; Muennighoff et al., 2022), as previously stated, much of the performance improvements in industrial use cases of embedding models stem from the prior data ingestion pipeline. While documents often rely on visual elements to more efficiently convey information to human readers, text-only systems barely tap into these visual cues.

To our knowledge, no benchmark evaluates document retrieval methods by considering both textual and visual document features like a human would.

2.2 Integrating Visual features

Contrastive Vision Language Models. Mapping latent representations of textual content to corresponding representations of visual content has been done by aligning disjoint visual and text encoders through contrastive losses (Radford et al., 2021; Zhai et al., 2023). While some OCR capabilities exist in these models, the visual component is often not optimized for text understanding. The Fine-grained Interactive Language-Image Pre-training (Yao et al., 2021) framework extends the late inter-

action mechanism to cross-modal vision-language models, relying on max similarity operations between text tokens and image patches.

Visually Rich Document Understanding. To go beyond text, some document-focused models jointly encode text tokens alongside visual or document layout features (Appalaraju et al., 2021; Kim et al., 2021; Huang et al., 2022; Tang et al., 2022). Large Language transformer Models (LLMs) with strong reasoning capabilities have recently been combined with Vision Transformers (ViTs) (Dosovitskiy et al., 2020) to create VLMs (Alayrac et al., 2022; Liu et al., 2023b; Bai et al., 2023; Laurençon et al., 2024) where image patch vectors from contrastively trained ViT models (Zhai et al., 2023) are fed as input embeddings to the language model and concatenated with the text-token embeddings.

PaliGemma. The PaliGemma-3B model (Lucas Beyer* et al., 2024) extends concepts from Pali3 (Chen et al., 2023), and projects SigLIP-So400m/14 (Alabdulmohsin et al., 2023) patch embeddings into Gemma-2B’s text vector space (Gemma Team et al., 2024). Along with its reasonable size w.r.t. other performant VLMs, an interesting property of PaliGemma’s text model is that it is fine-tuned with full-block attention on the prefix (instruction text and image tokens).

VLMs display enhanced capabilities in Visual Question Answering, captioning, and document understanding (Yue et al., 2023), but are not optimized for retrieval tasks.

3 The ViDoRe Benchmark

Existing benchmarks for contrastive vision-language models primarily evaluate retrieval for natural images (Lin et al., 2014; Borchmann et al., 2021; Thapliyal et al., 2022). On the other hand, textual retrieval benchmarks (Muennighoff et al., 2022) are evaluated at the textual passage level and are not tailored for document retrieval tasks. We fill the gap with *ViDoRe*, a comprehensive benchmark for document retrieval using visual features.

3.1 Benchmark Design

ViDoRe is designed to comprehensively evaluate retrieval systems on their capacity to match queries to relevant documents at the page level. This benchmark encompasses multiple orthogonal subtasks, with focuses on various modalities - text, figures, infographics, tables; thematic domains - medical, business, scientific, administrative; or languages -

English (eng), French (fra).

Dataset	# Queries	Domain
Academic Tasks		
DocVQA (eng)	500 (500)	Industrial
InfoVQA (eng)	500 (500)	Infographics
TAT-DQA (eng)	1600 (1600)	Varied Modalities
arXivVQA (eng)	500 (500)	Scientific Figures
TabFQuAD (fra)	210 (210)	Tables
Practical Tasks		
Energy (eng)	100 (1000)	Scientific
Government (eng)	100 (1000)	Administrative
Healthcare (eng)	100 (1000)	Medical
AI (eng)	100 (1000)	Scientific
Shift Project (fra)	100 (1000)	Environment

Table 1: *ViDoRe* comprehensively evaluates multimodal retrieval methods. The size of the document corpus is indicated in parentheses.

Academic Tasks. We repurpose widely used visual question-answering benchmarks for retrieval tasks: for each page-question-answer triplet, we use the question as the query, and the associated page as the gold document (Table 1). These academic datasets either focus on single specific modalities (Mathew et al., 2020, 2021; Li et al., 2024) or target more varied visually rich documents (Zhu et al., 2022). Moreover, we consider TabFQuAD, a human-labeled dataset on tables extracted from French industrial PDF documents released with this work. Details can be found in subsection A.1.

Practical tasks. We construct topic-specific retrieval benchmarks spanning multiple domains to go beyond repurposed QA datasets and evaluate retrieval in more realistic industrial situations (e.g. RAG). To achieve this, we collect publicly accessible PDF documents and generate queries pertaining to document pages using Claude-3 Sonnet, a high-quality proprietary vision-language model (Anthropic, 2024). In total, we collect 1,000 document pages per topic, which we associate with 100 queries extensively filtered for quality and relevance by human annotators. The corpus topics are intentionally specific to maximize syntactic proximity between documents, creating challenging retrieval tasks and covering an array of orthogonal domains (Table 1). Query-page pair examples are shown in Appendix E.²

Evaluation Metrics. We evaluate performance on our benchmark (Requirement R1) using standard metrics from the retrieval literature (NDCG, Re-

²Answers are generated alongside queries to (1) ground queries and improve their quality and (2) provide resources to foster future work.

call@K, MRR). We report NDCG@5 values as the main performance metric in this work and release the complete sets of results along with the models³. To validate compliance with practical industrial constraints, we also consider query latencies (R2) and indexing throughputs (R3).

3.2 Assessing Current Systems

Unstructured. We evaluate retrieval systems representative of those found in standard industrial RAG pipelines. As is common practice, we rely on the Unstructured⁴ off-the-shelf tool in the highest resolution settings to construct high-quality text chunks from PDF documents. Unstructured orchestrates the document parsing pipeline, relying on deep learning vision models to detect titles and document layouts (Ge et al., 2021), OCR engines (Smith, 2007) to extract text in non-native PDFs, specialized methods or models to detect and reconstruct tables, and implements a chunking strategy (`by-title`) that leverages the detected document structure to preserve section boundaries when concatenating texts. As is common practice, in our simplest Unstructured configuration (`text-only`), only textual elements are kept, and figures, images, and tables are considered noisy information and are filtered out.

Unstructured + X. While Unstructured is a strong baseline by itself, we further augment Unstructured’s output by integrating the visual elements. In (+ *OCR*), tables, charts, and images are run through an OCR engine, processed by Unstructured, and chunked independently. In (+ *Captioning*), we set up a fully-fledged captioning strategy (Zhao et al., 2023), in which we feed visual elements to a strong proprietary Vision Language Model (Claude-3 Sonnet (Anthropic, 2024)) to obtain highly detailed textual descriptions of the elements. Both strategies aim to integrate visual elements in the retrieval pipeline but incur significant latency and resource costs (subsection 5.2).

Embedding Model. To embed textual chunks, we evaluate Okapi BM25, the *de facto* standard sparse statistical retrieval method, and the dense encoder of BGE-M3 (Chen et al., 2024), a multilingual neural method with SOTA performance in its size category. Chunks are embedded and scored independently, and page-level scores are obtained by max-pooling over the page’s chunk scores.⁵

³<https://huggingface.co/vidore>

⁴www.unstructured.io

⁵We empirically validated the max-pooling strategy over

Contrastive VLMs. We also evaluate the strongest available vision-language embedding models; Jina CLIP (Koukounas et al., 2024), Nomic Embed Vision (Nomic, 2024), and SigLIP-So400m/14 (Alabdulmohsin et al., 2023).

Results. From a performance perspective, best results are obtained by combining the Unstructured parser with visual information, either from captioning strategies or by running OCR on the visual elements (Table 2). Little difference is seen between BM25 and BGE-M3 embeddings highlighting the visual information bottleneck. Contrastive VLMs lag behind. Beyond retrieval performance (R1), the indexing latencies (R2) reported in Figure 3 illustrate that PDF parsing pipelines can be very lengthy, especially when incorporating OCR or captioning strategies. Querying latencies at runtime (R3) are very good for all evaluated systems (≤ 22 ms on NVIDIA L4) due to fast query encoding and cosine similarity matching.

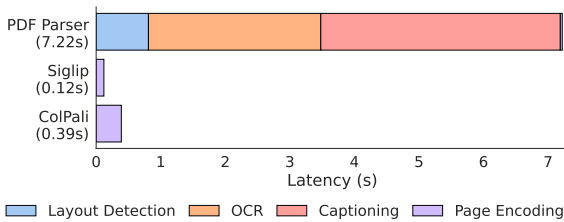


Figure 3: Offline indexing with *ColPali* is much simpler and faster compared to standard retrieval methods. Indexing speeds reported are computed on Nvidia L4 GPUs and detailed in subsection B.5.

4 Late interaction based Vision Retrieval

4.1 Architecture

Vision-Language Models. Encouraged by their strong document understanding capabilities, we propose adapting recent VLMs for retrieval. The key concept is to leverage the alignment between output embeddings of text and image tokens acquired during multi-modal finetuning. To this extent, we introduce **ColPali**, a PaliGemma-3B extension that is capable of generating ColBERT-style multi-vector representations of text and images (Figure 2). PaliGemma-3B is a strong candidate due to its small size, the many released checkpoints fine-tuned for different image resolutions and tasks, and the promising performances on various document understanding benchmarks. We add a pro-

sub-page chunks to be more effective than concatenating all page chunks before embedding pagewise.

jection layer to map the output language modeling embeddings to a vector space of reduced dimension $D = 128$ as used in the ColBERT paper (Khattab and Zaharia, 2020) to keep lightweight bag-of-embedding representations.

Late Interaction. Given query q and document d , we denote as $\mathbf{E}_q \in \mathbb{R}^{N_q \times D}$ and $\mathbf{E}_d \in \mathbb{R}^{N_d \times D}$ their respective multi-vector representation in the common embedding space \mathbb{R}^D . The late interaction operator, $\text{LI}(q, d)$, is the sum over all query vectors $\mathbf{E}_q^{(i)}$, of its maximum dot product $\langle \cdot | \cdot \rangle$ with each of the N_d document embedding vectors $\mathbf{E}_d^{(1:N_d)}$.

$$\text{LI}(q, d) = \sum_{i \in [1, N_q]} \max_{j \in [1, N_d]} \langle \mathbf{E}_q^{(i)} | \mathbf{E}_d^{(j)} \rangle \quad (1)$$

Contrastive Loss. The Late Interaction operation is fully differentiable, enabling backpropagation. Let a batch $\{q_k, d_k\}_{k \in [1, b]}$ composed of b query-page pairs, where for all $k \in [1, b]$, the document page d_k is the document corresponding to query q_k . Following Khattab and Zaharia (2020), we define our in-batch contrastive loss \mathcal{L} as the softmaxed cross-entropy of the positive scores $s_k^+ = \text{LI}(d_k, q_k)$ w.r.t. to the maximal negative scores $s_k^- = \max_{l, l \neq k} \text{LI}(q_k, p_l)$.

4.2 Model training

Dataset. Our training dataset of 127,460 query-page pairs is comprised of train sets of openly available academic datasets (63%) and a synthetic dataset made up of pages from web-crawled PDF documents and augmented with VLM-generated (Claude-3 Sonnet) pseudo-questions (37%). Our training set is fully English by design, enabling us to study zero-shot generalization to non-English languages⁶. We explicitly verify no multi-page PDF document is used both *ViDoRe* and in the train set to prevent evaluation contamination. A validation set is created with 2% of the samples to tune hyperparameters.

Parameters. All models are trained for 1 epoch on the train set. Unless specified otherwise, we train models in `bf16` format, use low-rank adapters (LoRA, Hu et al. (2021)) with $\alpha = 32$ and $r = 32$ on the transformer layers from the language model, as well as the final randomly initialized projection layer, and use a `paged_adamw_8bit` optimizer. We

⁶Multilingual data is present in the pretraining corpus of the language model (Gemma-2B) and potentially occurs during PaliGemma-3B’s multimodal training.

train on an 8 GPU setup with data parallelism, a learning rate of $5e - 5$ with linear decay with 2.5% warmup steps, and a batch size of 32.

Query Augmentation. As in [Khattab and Zaharia \(2020\)](#), we append 5 `<unused0>` tokens to the query tokens to serve as a soft, differentiable query expansion or re-weighting mechanism.

5 Results

5.1 Performance (R1)

We iteratively construct *ColPali*, starting from an off-the-shelf SigLIP model ([Table 2](#)).

BiSigLIP: Improving a strong model. SigLIP⁷ is a strong vision-language bi-encoder model, pre-trained on the English split of WebLI ([Chen et al., 2023](#)), a corpus of billions of image-text pairs. We find that SigLIP largely outperforms both Jina CLIP and Nomic-vision on document retrieval tasks. Further fine-tuning the textual component of this model on our document-oriented dataset (BiSigLIP) yields clear improvements across the board, particularly on figure retrieval (ArxivQA) and table retrieval tasks (TabFQuAD).

BiPali: Pairing with a language model. In the PaliGemma model architecture, SigLIP-generated patch embeddings are fed to a text language model to obtain LLM contextualized output patch embeddings.⁸ We average pool these representations to obtain a single dense vector, effectively creating a PaliGemma bi-encoder model (BiPali). After fine-tuning on the training dataset, we obtain a model that performs slightly worse in English than the tuned BiSigLIP variant. This can be explained by the fact that contrary to SigLIP, the original PaliGemma is not trained on contrastive matching tasks, but rather on next token prediction. Our contrastive fine-tuning phase on 100K images to transform PaliGemma into a bi-encoder is 5 orders of magnitude smaller than SigLIP’s original contrastive training. However, we see notable improvements in French tasks, indicating that BiPali’s LLM (Gemma 2B) helps multilingual text understanding. This is particularly notable as our training dataset does not contain non-English samples.

ColPali: Adding Late Interaction. One benefit of inputting image patch embeddings through a

language model is that they are natively mapped to a latent space similar to textual input (query). This enables leveraging the ColBERT strategy to compute interactions between text tokens and image patches, which enables a step-change improvement in performance compared to BiPali. Results in [Table 2](#) show that our *ColPali* model also largely outperforms the strong baselines based on Unstructured and captioning, as well as all evaluated text-image embedding models. The difference is particularly stark on the more visually complex benchmark tasks, such as InfographicVQA, ArxivQA, and TabFQuAD representing respectively infographics, figures, and tables. However, text-centric documents are also better retrieved by the *ColPali* models across all evaluated domains and languages, making our approach the overall best-performing document-retrieval model.

Negative Results. For extensiveness, we also train ColSigLIP, a late interaction variant of the BiSigLIP model but obtain abysmal performances. We attribute this to the large gaps w.r.t. SigLIP’s pre-training, in which only a pooled latent representation is used in the contrastive loss, which does not optimize the representations of individual patch and token embeddings. Similarly, we train a BiSigLIP_{PaliGemma} variant, in which we retrieve the image representations from the SigLIP model that has been further updated by PaliGemma fine-tuning, and use the text representations from PaliGemma’s text model. After fine-tuning on our dataset, performance is severely inferior to SigLIP_{Vanilla} which simply encodes with SigLIP’s original text and vision components. This indicates a logical misalignment between SigLIP embeddings, and Gemma embeddings after PaliGemma training. We detail these results in [Table 5](#).

5.2 Latencies & Memory Footprint

Online Querying. (R2) Logically, querying latencies differ between *ColPali* and a BGE-M3 embedding model. For BGE, encoding takes about 22 ms for 15 tokens, while encoding a query with *ColPali*’s language model takes about 30 ms⁹. For smaller corpus sizes, computing the late interaction operation induces marginally small overheads (≈ 1 ms per 1000 pages in the corpus), and the cosine similarity computation between bi-encoder vectors is even faster. Optimized late interaction engines ([Santhanam et al., 2022](#); [Lee et al., 2023](#)) enable to

⁷<https://huggingface.co/google/siglip-so400m-patch14-384>

⁸Note that the SigLIP model used in PaliGemma slightly differs in terms of number patches - 1024 patches for PaliGemma’s vision encoder, and 729 for the standalone SigLIP model.

⁹Computed for a batch size of 1 (online), and averaged over 1000 queries. See [subsection B.5](#)

	ArxivQ	DocQ	InfoQ	TabF	TATQ	Shift	AI	Energy	Gov.	Health.	Avg.
Unstructured <small>Text only</small>											
- BM25	-	34.1	-	-	44.0	59.6	90.4	78.3	78.8	82.6	-
- BGE-M3	-	28.4 _{↓5.7}	-	-	36.1 _{↓7.9}	68.5 _{↑8.9}	88.4 _{↓2.0}	76.8 _{↓1.5}	77.7 _{↓1.1}	84.6 _{↑2.0}	-
Unstructured <small>+ OCR</small>											
- BM25	31.6	36.8	62.9	46.5	62.7	64.3	92.8	85.9	83.9	87.2	65.5
- BGE-M3	31.4 _{↓0.2}	25.7 _{↓11.1}	60.1 _{↓2.8}	70.8 _{↑24.3}	50.5 _{↓12.2}	73.2 _{↑8.9}	90.2 _{↓2.6}	83.6 _{↓2.3}	84.9 _{↑1.0}	91.1 _{↑3.9}	66.1 _{↑0.6}
Unstructured <small>+ Captioning</small>											
- BM25	40.1	38.4	70.0	35.4	61.5	60.9	88.0	84.7	82.7	89.2	65.1
- BGE-M3	35.7 _{↓4.4}	32.9 _{↓5.4}	71.9 _{↑1.9}	69.1 _{↑33.7}	43.8 _{↓17.7}	73.1 _{↑12.2}	88.8 _{↑0.8}	83.3 _{↓1.4}	80.4 _{↓2.3}	91.3 _{↑2.1}	67.0 _{↑1.9}
Contrastive VLMs											
Jina-CLIP	25.4	11.9	35.5	20.2	3.3	3.8	15.2	19.7	21.4	20.8	17.7
Nomic-vision	17.1	10.7	30.1	16.3	2.7	1.1	12.9	10.9	11.4	15.7	12.9
SigLIP (Vanilla)	43.2	30.3	64.1	58.1	26.2	18.7	62.5	65.7	66.1	79.1	51.4
Ours											
SigLIP (Vanilla)	43.2	30.3	64.1	58.1	26.2	18.7	62.5	65.7	66.1	79.1	51.4
BiSigLIP (+fine-tuning)	58.5 _{↑15.3}	32.9 _{↑2.6}	70.5 _{↑6.4}	62.7 _{↑4.6}	30.5 _{↑4.3}	26.5 _{↑7.8}	74.3 _{↑11.8}	73.7 _{↑8.0}	74.2 _{↑8.1}	82.3 _{↑3.2}	58.6 _{↑7.2}
BiPali (+LLM)	56.5 _{↓-2.0}	30.0 _{↓-2.9}	67.4 _{↓-3.1}	76.9 _{↑14.2}	33.4 _{↑2.9}	43.7 _{↑17.2}	71.2 _{↓-3.1}	61.9 _{↓-11.7}	73.8 _{↓-0.4}	73.6 _{↓-8.8}	58.8 _{↑0.2}
<i>ColPali</i> (+Late Inter.)	79.1 _{↑22.6}	54.4 _{↑24.5}	81.8 _{↑14.4}	83.9 _{↑7.0}	65.8 _{↑32.4}	73.2 _{↑29.5}	96.2 _{↑25.0}	91.0 _{↑29.1}	92.7 _{↑18.9}	94.4 _{↑20.8}	81.3 _{↑22.5}

Table 2: **Comprehensive evaluation of baseline models and our proposed method on *ViDoRe*.** Results are presented using NDCG@5 metrics, and illustrate the impact of different components. Text-only metrics are not computed for benchmarks with only visual elements.

easily scale corpus sizes to millions of documents with reduced latency degradations.

Offline Indexing. (R3) Standard retrieval methods using bi-encoders represent each chunk as a single vector embedding, which is easy to store and fast to compute. However, processing a PDF to get the different chunks is the most time-consuming part (layout detection, OCR, chunking), and using captioning to handle multimodal data will only exacerbate this already lengthy process. On the other hand, *ColPali* directly encodes pages from their image representation. Although the encoder model is larger than standard retrieval encoders, skipping the preprocessing allows large speedups at indexing¹⁰ (Figure 3).

Memory Footprint. Our method requires storing a vector per image patch. We project each PaliGemma vector to a lower dimensional space (D=128) to maximize efficiency, leading to a memory footprint of 256 KB per page (subsection B.4). Importantly, the memory footprint of the naive ColBERT indexing strategy can be drastically improved through compression and clustering mechanisms as proposed in the Performance-optimized Late Interaction Driver (Santhanam et al., 2022).

¹⁰Measures a NVIDIA L4 GPU, averaged on 100 pages, with a batch size of 4 pages for *ColPali* and 8 text chunks for Bi-Encoders. On average, a page is divided into 2.1 chunks. See subsection B.5.

5.3 Interpretability

By superimposing the late interaction heatmap on top of the original image, we can visualize the most salient image patches with respect to each term of the query, yielding interpretable insights into model focus zones. As epitomized in Figure 1, we observe *ColPali* exhibits strong OCR capabilities as both the words "hourly" and "hours" present a high similarity score with the query token <_hour>. We also note particular focus on other non-trivial image features such as the x-axis representing hours being salient. Other visualization examples with similar trends of the model transcending pure OCR are shown in Appendix C.

6 Ablation study

Should we scale models or patch numbers ?

We train a variant of PaliGemma with half the number of image patches (512). While there is a clear performance degradation w.r.t. to the 1024-patch *ColPali* model (Figure 4), memory usage is much lower.¹¹ As an alternative to PaliGemma, we train Idefics2-8B (Laurençon et al., 2024), a VLM with a similar architecture and based on a Mistral-7B

¹¹While another PaliGemma variant exists with 2048 patches, the different training datamix and the large memory requirements make this model impractical for both training and inference time.

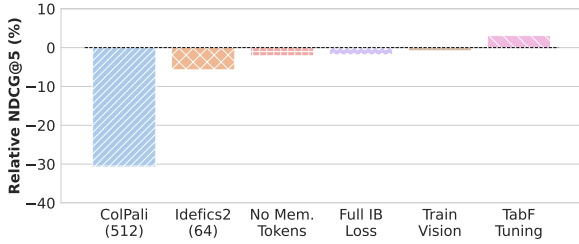


Figure 4: Relative NDCG@5 performance gain w.r.t. the default *ColPali* (1024 patches). *TabFQuAD fine-tuning* measures the performance difference on the TabFQuAD task after the introduction of targeted data in the training set. All other results refer to performance deltas averaged on all *ViDoRe* tasks.

(Jiang et al., 2023) language backbone and a SigLIP vision encoder paired with a perceiver resampler. The most notable differences with PaliGemma lie in the size of the language model (2B and 7B resp.) and the number of image patches (between 512 and 2048 for PaliGemma, and 60 post-resampling for Idefics2¹²). Our results (Figure 4) suggest language model size has a strong impact on performance, and along with the trained resampler enables more efficient representations for smaller numbers of image embeddings - ColIdefics2 with 60 patches edges out *ColPali* with 512 patches. Scaling the number of patches of the smaller *ColPali* model from 512 to 1024, enables largely surpassing the 60-patch ColIdefics2 while being about twice as fast in terms of training and inference latency. These results suggest there are *tradeoffs* between performance (R1), latencies during online querying (R2) and offline indexation phases (R3), and index memory size.

Should we fine-tune the vision component?

We run our contrastive finetuning on a *ColPali* model in which we also train the vision encoder and the projection layer. Results in Figure 4 show this leads to no significant improvements.

Do "query augmentation" tokens help?

In ColBERT, special tokens are concatenated to the input query to serve as soft query augmentation buffers. Training without these tokens, we observe no significant performance difference (Figure 4) in the English benchmarks. However, performance on the French tasks seems to improve (Table 5)

Is the Pairwise CE loss best?

Training with an in-batch negative contrastive loss,

¹²With the option of adding 4 sub-image crops of 64 tokens each to the sequence, for a total of 320 tokens

instead of the pairwise CE loss that only considers the hardest negative sample, leads to a slight performance degradation (-2.4%) on the aggregated benchmark.

Can the model adapt to new tasks?

Contrary to more complex multi-step retrieval pipelines, *ColPali* can be trained end-to-end, directly optimizing the downstream retrieval task which greatly facilitates fine-tuning to boost performance on specialized domains, multilingual retrieval, or specific visual elements the model struggles with. To demonstrate, we add 1552 samples representing French tables and associated queries to the training set. This represents the only French data in the training set, with all other examples being kept unchanged. We see significant NDCG@5 improvements (Figure 4) and even starker Recall@1 gains (+6.63%) on the TabFQuAD benchmark, with no performance degradation on the rest of the benchmark tasks (+0.34%).

7 Conclusions

Through the conception of a new benchmark *ViDoRe*, we established the limits of both modern industrial document retrieval pipelines and off-the-shelf image-text contrastive models for visually rich document retrieval. We introduced *ColPali*, a novel retrieval model that leverages the latest generative Vision Language models to create highly performing multi-vector embeddings purely from visual document features. *ColPali* largely outperforms the best existing document retrieval methods while enabling faster corpus indexing time and maintaining low querying latencies, suggesting a very high potential for industrial document retrieval applications. We hope to encourage future work by publicly releasing the *ViDoRe* benchmark and all models and baselines from our study.

Future Work. Further performance gains could be obtained by exploring sub-image decomposition (Liu et al., 2023a), optimal image patch resampling strategies (Laurençon et al., 2024), or hard-negative mining. Subsequently, our vision is to combine visual retrieval and visually grounded query answering to create RAG systems that purely function from visual features. An interesting line of research could be attempting to generate answers leveraging information stored in the indexed multi-vector patch embeddings.

Limitations

Focus. In this work, we evaluate models on document retrieval tasks, covering several modalities (figures, text, tables, infographics). We however primarily focus on PDF-type documents, and evaluating systems on image retrieval with documents stemming from web page screenshots or handwritten documents might be an interesting generalization. We also focus on high-resource languages (English and French) and although we have shown the capacity of the *ColPali* model to generalize to languages outside of its fine-tuning set, it is unclear how the model would perform on languages that are not as represented in the model’s language backbone. Finally, our setup assumes relevant documents exist, but abstention methods for Information Retrieval systems might be interesting to explore in more practical settings in which confidence estimation might be important (Gisserot-Boukhlef et al., 2024).

Support. This work relies on multi-vector retrieving derived from the ColBERT late interaction mechanism. Although some vector databases support late interaction engines¹³, many widely used vector retrieval frameworks do not propose native multi-vector support, and some engineering infrastructure efforts may be required to adapt them to work with *ColPali* (or ColBERT) models.

Data. In the creation of *ViDoRe*, we partially rely on synthetic query generation based on a commercial large language model, which may induce some amount of bias in the generated queries. To compensate for this, we have iterated on the prompting strategy and given real query examples to the models to help ground generation in realistic settings. We have further manually verified all synthetic queries through a lengthy process to validate their relevance and their quality. Our benchmark also includes many benchmark tasks with no synthetic data, and result trends observed between all tasks are correlated, further confirming the coherence of our benchmark design.

Ethical Considerations

Carbon Footprint. Our work fully leverages prior pretrained models and training is not particularly compute-intensive. Furthermore, we rely on low-rank adapters to further reduce the computational resources needed, both during training and for

storage. Overall, a training run represents about 40 hours of Mi250x AMD GPUs. Our experiments, in total, represent 1405 Mi250x GPU hours from highly efficient compute clusters running on low-carbon nuclear energy, representing a total of around 15kg CO2 eq.

Impact. We believe our work could have a strong impact on improving industrial document retrieval systems. Our method is efficient, performs well, and the additional support towards visually rich information from documents could go a long way in unlocking knowledge sources previously difficult to index or query.

Resource Release. For transparency, and to foster future work, we release our comprehensive benchmark under open license and host a public leaderboard¹⁴. Our models are released under the same usage license as the base model (Gemma Research license for ColPali, Apache2.0 for ColDefics2) and should be used as intended by the VLM license.

Acknowledgements

This work is partially supported by Illuin Technology, and by a grant from ANRT France. This work was performed using HPC resources from the CINES ADASTRA through Grant 2024-AD011015443. We extend our warm thanks to Jonathan Dong, Caio Corro, Victor Pellegrain and Ender Konukoglu for their valuable feedback on the paper.

References

- Ibrahim Alabdulmohsin, Xiaohua Zhai, Alexander Kolesnikov, and Lucas Beyer. 2023. *Getting ViT in Shape: Scaling Laws for Compute-Optimal Model Design*. Publisher: arXiv Version Number: 5.
- Jean-Baptiste Alayrac, Jeff Donahue, Pauline Luc, Antoine Miech, Iain Barr, Yana Hasson, Karel Lenc, Arthur Mensch, Katie Millican, Malcolm Reynolds, Roman Ring, Eliza Rutherford, Serkan Cabi, Tengda Han, Zhitao Gong, Sina Samangooei, Marianne Monteiro, Jacob Menick, Sebastian Borgeaud, Andrew Brock, Aida Nematzadeh, Sahand Sharifzadeh, Mikolaj Binkowski, Ricardo Barreira, Oriol Vinyals, Andrew Zisserman, and Karen Simonyan. 2022. *Flamingo: a Visual Language Model for Few-Shot Learning*. Publisher: arXiv Version Number: 2.
- Anthropic. 2024. *The Claude 3 Model Family: Opus, Sonnet, Haiku*.

¹³Vespa Engine, RAGatouille, QDrant, colbert.ai

¹⁴<https://huggingface.co/spaces/vidore/vidore-leaderboard>

- Srikar Appalaraju, Bhavan Jasani, Bhargava Urala Kota, Yusheng Xie, and R. Manmatha. 2021. [DocFormer: End-to-End Transformer for Document Understanding](#). *arXiv preprint*. Version Number: 2.
- Jinze Bai, Shuai Bai, Shusheng Yang, Shijie Wang, Sinan Tan, Peng Wang, Junyang Lin, Chang Zhou, and Jingren Zhou. 2023. [Qwen-VL: A Versatile Vision-Language Model for Understanding, Localization, Text Reading, and Beyond](#). Publisher: arXiv Version Number: 3.
- Payal Bajaj, Daniel Campos, Nick Craswell, Li Deng, Jianfeng Gao, Xiaodong Liu, Rangan Majumder, Andrew McNamara, Bhaskar Mitra, Tri Nguyen, Mir Rosenberg, Xia Song, Alina Stoica, Saurabh Tiwary, and Tong Wang. 2016. [MS MARCO: A Human Generated MACHine Reading COmprehension Dataset](#). *arXiv preprint*. Version Number: 3.
- Burton H. Bloom. 1970. [Space/time trade-offs in hash coding with allowable errors](#). *Commun. ACM*, 13(7):422–426. Place: New York, NY, USA Publisher: Association for Computing Machinery.
- Łukasz Borchmann, Michał Pietruszka, Tomasz Stanisławek, Dawid Jurkiewicz, Michał Turski, Karolina Szyndler, and Filip Galiński. 2021. [DUE: End-to-End Document Understanding Benchmark](#). In *Thirty-fifth Conference on Neural Information Processing Systems Datasets and Benchmarks Track (Round 2)*.
- Jianlv Chen, Shitao Xiao, Peitian Zhang, Kun Luo, Defu Lian, and Zheng Liu. 2024. [BGE M3-Embedding: Multi-Lingual, Multi-Functionality, Multi-Granularity Text Embeddings Through Self-Knowledge Distillation](#). *arXiv preprint*. Version Number: 3.
- Xi Chen, Xiao Wang, Lucas Beyer, Alexander Kolesnikov, Jialin Wu, Paul Voigtlaender, Basil Mustafa, Sebastian Goodman, Ibrahim Alabdulmohsin, Piotr Padlewski, Daniel Salz, Xi Xiong, Daniel Vlasic, Filip Pavetic, Keran Rong, Tianli Yu, Daniel Keysers, Xiaohua Zhai, and Radu Soricut. 2023. [PaLI-3 Vision Language Models: Smaller, Faster, Stronger](#). *arXiv preprint*. Version Number: 2.
- Cohere. 2024. [Introducing Rerank 3: A New Foundation Model for Efficient Enterprise Search & Retrieval](#).
- Timothée Darcet, Maxime Oquab, Julien Mairal, and Piotr Bojanowski. 2023. [Vision Transformers Need Registers](#). Publisher: [object Object] Version Number: 2.
- Alexey Dosovitskiy, Lucas Beyer, Alexander Kolesnikov, Dirk Weissenborn, Xiaohua Zhai, Thomas Unterthiner, Mostafa Dehghani, Matthias Minderer, Georg Heigold, Sylvain Gelly, Jakob Uszkoreit, and Neil Houlsby. 2020. [An Image is Worth 16x16 Words: Transformers for Image Recognition at Scale](#). Publisher: arXiv Version Number: 2.
- Zheng Ge, Songtao Liu, Feng Wang, Zeming Li, and Jian Sun. 2021. [YOLOX: Exceeding YOLO Series in 2021](#). *arXiv preprint*. Version Number: 2.
- Gemma Team, Thomas Mesnard, Cassidy Hardin, Robert Dadashi, Surya Bhupatiraju, Shreya Pathak, Laurent Sifre, Morgane Rivière, Mihir Sanjay Kale, Juliette Love, Pouya Tafti, Léonard Hussenot, Pier Giuseppe Sessa, Aakanksha Chowdhery, Adam Roberts, Aditya Barua, Alex Botev, Alex Castro-Ros, Ambrose Slone, Amélie Héliou, Andrea Tacchetti, Anna Bulanova, Antonia Paterson, Beth Tsai, Bobak Shahriari, Charline Le Lan, Christopher A. Choquette-Choo, Clément Crepy, Daniel Cer, Daphne Ippolito, David Reid, Elena Buchatskaya, Eric Ni, Eric Noland, Geng Yan, George Tucker, George-Christian Muraru, Grigory Rozhdestvenskiy, Henryk Michalewski, Ian Tenney, Ivan Grishchenko, Jacob Austin, James Keeling, Jane Labanowski, Jean-Baptiste Lespiau, Jeff Stanway, Jenny Brennan, Jeremy Chen, Johan Ferret, Justin Chiu, Justin Mao-Jones, Katherine Lee, Kathy Yu, Katie Millican, Lars Lowe Sjoesund, Lisa Lee, Lucas Dixon, Machel Reid, Maciej Mikuła, Mateo Wirth, Michael Sharman, Nikolai Chinaev, Nithum Thain, Olivier Bachem, Oscar Chang, Oscar Wahltinez, Paige Bailey, Paul Michel, Petko Yotov, Rahma Chaabouni, Ramona Comanescu, Reena Jana, Rohan Anil, Ross McIlroy, Ruibo Liu, Ryan Mullins, Samuel L Smith, Sebastian Borgeaud, Sertan Girgin, Sholto Douglas, Shree Pandya, Siamak Shakeri, Soham De, Ted Klimenko, Tom Hennigan, Vlad Feinberg, Wojciech Stokowiec, Yu-hui Chen, Zafarali Ahmed, Zhitao Gong, Tris Warkentin, Ludovic Peran, Minh Giang, Clément Farabet, Oriol Vinyals, Jeff Dean, Koray Kavukcuoglu, Demis Hassabis, Zoubin Ghahramani, Douglas Eck, Joelle Barral, Fernando Pereira, Eli Collins, Armand Joulin, Noah Fiedel, Evan Senter, Alek Andreev, and Kathleen Kenealy. 2024. [Gemma: Open Models Based on Gemini Research and Technology](#). *arXiv preprint*. Version Number: 4.
- Hippolyte Gisserot-Boukhlef, Manuel Faysse, Emmanuel Malherbe, Céline Hudelot, and Pierre Colombo. 2024. [Towards trustworthy reranking: A simple yet effective abstention mechanism](#). *Preprint*, arXiv:2402.12997.
- Edward J. Hu, Yelong Shen, Phillip Wallis, Zeyuan Allen-Zhu, Yuanzhi Li, Shean Wang, Lu Wang, and Weizhu Chen. 2021. [LoRA: Low-Rank Adaptation of Large Language Models](#). Publisher: arXiv Version Number: 2.
- Yupan Huang, Tengchao Lv, Lei Cui, Yutong Lu, and Furu Wei. 2022. [LayoutLMv3: Pre-training for Document AI with Unified Text and Image Masking](#). Publisher: arXiv Version Number: 3.
- Albert Q. Jiang, Alexandre Sablayrolles, Arthur Mensch, Chris Bamford, Devendra Singh Chaplot, Diego de las Casas, Florian Bressand, Gianna Lengyel, Guillaume Lample, Lucile Saulnier, Léo Renard Lavaud, Marie-Anne Lachaux, Pierre Stock, Teven Le Scao, Thibaut Lavril, Thomas Wang, Timothée Lacroix,

- and William El Sayed. 2023. [Mistral 7B](#). Publisher: arXiv Version Number: 1.
- Vladimir Karpukhin, Barlas Oğuz, Sewon Min, Patrick Lewis, Ledell Wu, Sergey Edunov, Danqi Chen, and Wen-tau Yih. 2020. [Dense Passage Retrieval for Open-Domain Question Answering](#). *arXiv preprint*. Version Number: 3.
- Omar Khattab and Matei Zaharia. 2020. [ColBERT: Efficient and Effective Passage Search via Contextualized Late Interaction over BERT](#).
- Geewook Kim, Teakgyu Hong, Moonbin Yim, Jeongyeon Nam, Jinyoung Park, Jinyeong Yim, Wonseok Hwang, Sangdoon Yun, Dongyoon Han, and Seunghyun Park. 2021. [OCR-free Document Understanding Transformer](#). *arXiv preprint*. Version Number: 5.
- Andreas Koukounas, Georgios Mastrapas, Michael Günther, Bo Wang, Scott Martens, Isabelle Mohr, Saba Sturua, Mohammad Kalim Akram, Joan Fontanals Martínez, Saahil Ognawala, Susana Guzman, Maximilian Werk, Nan Wang, and Han Xiao. 2024. [Jina CLIP: Your CLIP Model Is Also Your Text Retriever](#). *arXiv preprint*. Version Number: 1.
- Hugo Laurençon, Léo Tronchon, Matthieu Cord, and Victor Sanh. 2024. [What matters when building vision-language models?](#) *arXiv preprint*. ArXiv:2405.02246 [cs].
- Jinhyuk Lee, Zhuyun Dai, Sai Meher Karthik Duddu, Tao Lei, Iftekhar Naim, Ming-Wei Chang, and Vincent Y. Zhao. 2023. [Rethinking the Role of Token Retrieval in Multi-Vector Retrieval](#). *arXiv preprint*. Version Number: 3.
- Lei Li, Yuqi Wang, Runxin Xu, Peiyi Wang, Xiachong Feng, Lingpeng Kong, and Qi Liu. 2024. [Multimodal arxiv: A dataset for improving scientific comprehension of large vision-language models](#). *Preprint*, arXiv:2403.00231.
- Tsung-Yi Lin, Michael Maire, Serge Belongie, Lubomir Bourdev, Ross Girshick, James Hays, Pietro Perona, Deva Ramanan, C. Lawrence Zitnick, and Piotr Dollár. 2014. [Microsoft COCO: Common Objects in Context](#). *arXiv preprint*. Version Number: 3.
- Haotian Liu, Chunyuan Li, Yuheng Li, and Yong Jae Lee. 2023a. [Improved Baselines with Visual Instruction Tuning](#). *arXiv preprint*. Version Number: 2.
- Haotian Liu, Chunyuan Li, Qingyang Wu, and Yong Jae Lee. 2023b. [Visual Instruction Tuning](#). Publisher: arXiv Version Number: 1.
- Lucas Beyer*, Andreas Steiner*, André Susano Pinto*, Alexander Kolesnikov*, Xiao Wang*, Xiaohua Zhai*, Daniel Salz, Maxim Neumann, Ibrahim Alabdulmohsin, Michael Tschannen, Jeremiah Harmsen, Daniel Keysers, Neil Houlsby, Xi Chen, Emanuele Bugliarello, Thomas Unterthiner, Keran Rong, Matthias Minderer, Ioana Bica, Ivana Balazevic, Joan Puigcerver, Julian Eisenschlos, Manoj Kumar, Matko Bošnjak, Matthias Bauer, Fangyu Liu, Adam Grycner, Alexey Gritsenko, Paul Voigtlaender, Pinelopi Papalampidi, Olivier Henaff, Skanda Koppala, Xi Xiong, Radu Soricut, Model release contributors and general support, Tris Warkentin, Kat Black, Luiz Gustavo Martins, Glenn Cameron, Raj Gundluru, Manvinder Singh, Meg Risdal, Nilay Chauhan, Nate Keating, Nesh Devanathan, Elisa Bandy, Joe Fernandez, Antonia Paterson, Jenny Brennan, Tom Eccles, Pankil Botadra, Ben Bariach, Lav Rai, Minwoo Park, Dustin Luong, Daniel Vlasic, Bo Wu, Wenming Ye, Divyashree Sreepathihalli, Kiranbir Sodhia, Alek Andreev, Armand Joulin, Surya Bhupatiraju, Minh Giang, Joelle Barral, and Zoubin Ghahramani. 2024. [PaliGemma](#).
- Minesh Mathew, Viraj Bagal, Rubèn Pérez Tito, Dimosthenis Karatzas, Ernest Valveny, and C. V. Jawahar. 2021. [InfographicVQA](#). *arXiv preprint*. Version Number: 2.
- Minesh Mathew, Dimosthenis Karatzas, and C. V. Jawahar. 2020. [DocVQA: A Dataset for VQA on Document Images](#).
- Niklas Muennighoff, Nouamane Tazi, Loïc Magne, and Nils Reimers. 2022. [MTEB: Massive Text Embedding Benchmark](#). *arXiv preprint*. Version Number: 3.
- Nomic. 2024. [Nomic Embed Vision: Expanding The Nomic Latent Space](#).
- Alec Radford, Jong Wook Kim, Chris Hallacy, Aditya Ramesh, Gabriel Goh, Sandhini Agarwal, Girish Sastry, Amanda Askell, Pamela Mishkin, Jack Clark, Gretchen Krueger, and Ilya Sutskever. 2021. [Learning Transferable Visual Models From Natural Language Supervision](#). Publisher: arXiv Version Number: 1.
- Nils Reimers and Iryna Gurevych. 2019. [Sentence-BERT: Sentence Embeddings using Siamese BERT-Networks](#). *arXiv preprint*. Version Number: 1.
- Stephen E. Robertson, Steve Walker, Susan Jones, Micheline Hancock-Beaulieu, and Mike Gatford. 1994. [Okapi at TREC-3](#). In *Proceedings of The Third Text REtrieval Conference, TREC 1994, Gaithersburg, Maryland, USA, November 2-4, 1994*, volume 500-225 of *NIST Special Publication*, pages 109–126. National Institute of Standards and Technology (NIST).
- Keshav Santhanam, Omar Khattab, Christopher Potts, and Matei Zaharia. 2022. [PLAID: An Efficient Engine for Late Interaction Retrieval](#). *arXiv preprint*. Version Number: 1.
- R. Smith. 2007. [An Overview of the Tesseract OCR Engine](#). In *Ninth International Conference on Document Analysis and Recognition (ICDAR 2007) Vol 2*, pages 629–633, Curitiba, Parana, Brazil. IEEE. ISSN: 1520-5363.

Karen Sparck Jones. 1972. [A STATISTICAL INTERPRETATION OF TERM SPECIFICITY AND ITS APPLICATION IN RETRIEVAL](#). *Journal of Documentation*, 28(1):11–21.

Zineng Tang, Ziyi Yang, Guoxin Wang, Yuwei Fang, Yang Liu, Chenguang Zhu, Michael Zeng, Cha Zhang, and Mohit Bansal. 2022. [Unifying Vision, Text, and Layout for Universal Document Processing](#). *arXiv preprint*. Version Number: 3.

Nandan Thakur, Nils Reimers, Andreas Rücklé, Abhishek Srivastava, and Iryna Gurevych. 2021. [BEIR: A Heterogenous Benchmark for Zero-shot Evaluation of Information Retrieval Models](#). *arXiv preprint*. Version Number: 4.

Ashish V. Thapliyal, Jordi Pont-Tuset, Xi Chen, and Radu Soricut. 2022. [Crossmodal-3600: A Massively Multilingual Multimodal Evaluation Dataset](#). *arXiv preprint*. Version Number: 2.

Liang Wang, Nan Yang, Xiaolong Huang, Binxing Jiao, Linjun Yang, Daxin Jiang, Rangan Majumder, and Furu Wei. 2022. [Text Embeddings by Weakly-Supervised Contrastive Pre-training](#). *arXiv preprint*. Version Number: 2.

Wenhui Wang, Furu Wei, Li Dong, Hangbo Bao, Nan Yang, and Ming Zhou. 2020. [MiniLM: Deep Self-Attention Distillation for Task-Agnostic Compression of Pre-Trained Transformers](#). *arXiv preprint*. ArXiv:2002.10957 [cs].

Lewei Yao, Runhui Huang, Lu Hou, Guansong Lu, Minzhe Niu, Hang Xu, Xiaodan Liang, Zhenguo Li, Xin Jiang, and Chunjing Xu. 2021. [FILIP: Fine-grained Interactive Language-Image Pre-Training](#). *arXiv preprint*. Version Number: 1.

Xiang Yue, Yuansheng Ni, Kai Zhang, Tianyu Zheng, Ruoqi Liu, Ge Zhang, Samuel Stevens, Dongfu Jiang, Weiming Ren, Yuxuan Sun, Cong Wei, Botao Yu, Ruibin Yuan, Renliang Sun, Ming Yin, Boyuan Zheng, Zhenzhu Yang, Yibo Liu, Wenhao Huang, Huan Sun, Yu Su, and Wenhui Chen. 2023. [MMMU: A Massive Multi-discipline Multimodal Understanding and Reasoning Benchmark for Expert AGI](#). *arXiv preprint*. Version Number: 3.

Xiaohua Zhai, Basil Mustafa, Alexander Kolesnikov, and Lucas Beyer. 2023. [Sigmoid Loss for Language Image Pre-Training](#). Publisher: [object Object] Version Number: 4.

Ruochen Zhao, Hailin Chen, Weishi Wang, Fangkai Jiao, Xuan Long Do, Chengwei Qin, Bosheng Ding, Xiaobao Guo, Minzhi Li, Xingxuan Li, and Shafiq Joty. 2023. [Retrieving Multimodal Information for Augmented Generation: A Survey](#). *arXiv preprint*. Version Number: 3.

Fengbin Zhu, Wenqiang Lei, Fuli Feng, Chao Wang, Haozhou Zhang, and Tat-Seng Chua. 2022. [Towards Complex Document Understanding By Discrete Reasoning](#). Publisher: arXiv Version Number: 3.

A Benchmark Datasets

A.1 Academic Datasets

DocVQA (Mathew et al., 2020) includes collected images from the UCSF Industry Documents Library. Questions and answers were manually annotated.

InfoVQA (Mathew et al., 2021) includes infographics collected from the Internet using the search query “*infographics*”. Questions and answers were manually annotated.

TAT-DQA (Zhu et al., 2022) is a large-scale Document VQA dataset that was constructed from publicly available real-world financial reports. It focuses on rich tabular and textual content requiring numerical reasoning. Questions and answers were manually annotated by human experts in finance.

arXivQA (Li et al., 2024) is a VQA dataset based on figures extracted from arXiv publications. The questions were generated synthetically using GPT-4 Vision.

TabFQuAD (Table French Question Answering Dataset) is designed to evaluate TableQA models in realistic industry settings. We create additional queries to augment the existing human-annotated ones using the same method described in [subsection A.2](#).

A.2 Practical Datasets

Methodology. Creating a relevant retrieval dataset close to real use cases is a major challenge as the dataset needs to be both sufficiently large for effective fine-tuning and sufficiently diverse to cover a broad range of modalities (full text, tables, charts, ...), domains (industry, healthcare, ...), and query-document interactions (extractive questions, open-ended questions, ...). Our approach to building this dataset involves several steps: (1) we use a web crawler to collect publicly available documents on various themes and sources, (2) we convert these PDFs into a series of images, one per page, and (3) we generate queries related to each image using a VLM.

Web-Crawler. We implemented a web crawler to efficiently collect large volumes of documents related to a given topic. The crawler is seeded with a user-defined query (e.g. “artificial intelligence”) and then uses GPT-3.5 Turbo to brainstorm related topics and subtopics. This query augmentation strategy aims at both broadening and deepening the search. GPT-3.5 Turbo is further used to generate diverse search queries from each subtopic. This

query set is then consumed by a pool of parallel workers whose job is to fetch the associated most relevant documents. We use SerpAPI¹⁵ along with a filetype filter (PDF documents only) to programmatically scrape Google Search rankings. Each file is hashed and stored in a Bloom filter (Bloom, 1970) shared among workers to avoid duplicate documents in the final corpus. Unique scraped files are downloaded, and inserted into a SQLite database along with additional metadata.

Datamix. Using the web crawler, we collected approximately 1,000 documents for each of the following four seeds: "energy", "government reports", "healthcare industry", and "artificial intelligence". These seeds were meticulously hand-picked to align with real-use cases for retrieval models and visually rich pages. We also removed all documents containing any private information. At this stage, we randomly selected 900 files for the training set and 100 files for the test set, ensuring that data leakage into the test set was avoided during subsequent processing steps.

Query Generation. To increase the efficiency of our query generation scheme and to limit API calls, we generate at most 3 questions per image. From all the documents collected, we randomly sample 10,000 images per theme and call Claude-3 Sonnet with the following prompt:

```
You are an assistant specialized in
↪ Multimodal RAG tasks.\n
The task is the following: given an image
↪ from a pdf page, you will have to
generate questions that can be asked by a
↪ user to retrieve information from
a large documentary corpus.
The question should be relevant to the
↪ page, and should not be too specific
or too general. The question should be
↪ about the subject of the page, and
the answer needs to be found in the page.
↪ \n
```

```
Remember that the question is asked by a
↪ user to get some information from a
large documentary corpus that contains
↪ multimodal data. Generate a question
that could be asked by a user without
↪ knowing the existence and the content
of the corpus. \n
Generate as well the answer to the
↪ question, which should be found in the
page. And the format of the answer should
↪ be a list of words answering the
question. \n
```

```
Generate at most THREE pairs of questions
↪ and answers per page in a
dictionary with the following format,
↪ answer ONLY this dictionary
NOTHING ELSE: \n
```

```
{
  "questions": [
    {
      "question": "XXXXXX",
      "answer": ["YYYYYY"]
    },
    {
      "question": "XXXXXX",
      "answer": ["YYYYYY"]
    },
    {
      "question": "XXXXXX",
      "answer": ["YYYYYY"]
    }
  ]
}
```

```
where XXXXXX is the question and
↪ ['YYYYYY'] is the corresponding list
↪ of answers
that could be as long as needed. \n
```

```
Note: If there are no questions to ask
↪ about the page, return an empty list.
Focus on making relevant questions
↪ concerning the page. \n
Here is the page: \n
```

Human Validation. We manually validate every single synthetically created query in *ViDoRe* to ensure quality, query relevance, and consistency with the benchmark objective of evaluating retrieval in practical industrial settings. During this step, we randomly assign document-pair queries to 4 vol-

¹⁵<https://serpapi.com/>

unteer annotators and instruct them to filter out queries that do not fit the above-listed criteria. We also instruct annotators to flag any documents they deem to contain PII information or content not suited for an academic benchmark. No flag was raised during the entirety of the process, validating our prior PDF collection strategy. 100 queries per topic are collected in this manner. Annotators are colleagues and collaborators of the authors who volunteered to help. Each annotator spent approximately 3 hours filtering the larger query set down to 100 high-quality queries per topic.

B Implementation details

B.1 Codebase

The codebase is written in PyTorch¹⁶ and leverages HuggingFace tooling for model implementations and trainers¹⁷.

B.2 Pairwise CE loss

Our in-batch contrastive loss \mathcal{L} is defined as the softmaxed cross-entropy of the positive scores $s_k^+ = \text{LI}(d_k, q_k)$ w.r.t. to the maximal negative scores $s_k^- = \max_{l, l \neq k} \text{LI}(q_k, p_l)$.

For numerical stability, we reformulate the loss with the softplus function, leading to:

$$\mathcal{L} = \frac{1}{b} \sum_{k=1}^b \text{softplus}(s_k^- - s_k^+) \quad (2)$$

B.3 Hyperparameters

Hyperparameters are tuned on a validation split composed of 2% of the training dataset. We find bi-encoder methods to be more sensible to learning rate variations than late interaction-based models and achieve the best performance for all models with a learning rate of $5e - 5$. We experiment with LoRA rank and α values and do not notice particular improvements past $r = \alpha = 32$. Per-device batch sizes are kept small due to long sequence lengths that complicate scaling past $b = 4$. Simulating larger batch sizes for in-batch negative sampling should enable even better results. We find the best results with global batch size $b = 32$ for 1 epoch on our training set.

B.4 Embedding size

Minimizing storage footprint can be essential to industrial retrieval systems if databases contain mil-

lions of documents. With this criterion in view, we have compared the embedding sizes of the models in our study. As shown in Table 3, *ColPali*'s embedding size is an order of magnitude larger than BM25 and two orders of magnitude larger than BGE-M3. However, this study is limited to the naive method of storing *ColPali*'s multi-vector embeddings. In practical scenarios, using cluster centroids can reduce the size of *ColPali* multi-vector embeddings by up to an order of magnitude (Santhanam et al., 2022) and make it a competitive retrieval system.

Model	Embedding size (KB)
BGE-M3	8.60
BM25 (dense emb.)	3.00
BM25 (sparse emb.)	1.56 ± 0.51
<i>ColPali</i> (float16)	256

Table 3: Comparison of the embedding sizes for the DocVQA test set from *ViDoRe* w.r.t. different retrieval models. The lower the size the smaller the storage footprint of the model. The *mean ± std* size is given for the sparse embeddings.

B.5 Latency computations

All latency computations are done on a NVIDIA L4 GPU. Queries are encoded independently (batch size of 1) to simulate online querying, and pages are encoded with a batch size of 4 for PaliGemma derived models, and 8 for BGE-M3. Reported times include image and text processing time before the model forward pass, as well as query-to-index matching times. We note an interesting feature of *ColPali* is that all documents have the same sequence length, leading to prior knowledge of runtime and memory consumptions. Query latency experiments are averaged over 1000 queries, and indexing times are measured for a 100 page document. Per page time is obtained by dividing total time by 100, corresponding to inverse page throughput.

B.6 Captioning

Examples of captions generated for visually rich document chunks with Claude-3 Sonnet are shown in Figure 6 and Figure 5. The prompt used for generating the description is the following:

¹⁶<https://pytorch.org/>

¹⁷<https://huggingface.co>

You are an assistant specialized in document analysis. Given a table or a figure, you have to provide a detailed summary of the content in maximum 3000 characters. Your summary should be qualitative and not quantitative. Here is the table/figure to analyze: {image}. Answer ONLY with the caption of the table/figure.

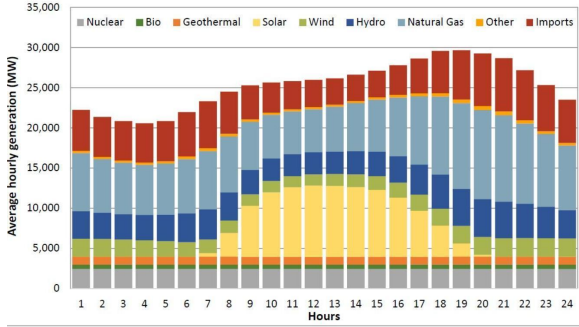


Figure 5: Example from the "Energy" test set.
Caption: The image depicts the hourly energy generation profile, illustrating the contributions of various energy sources over 24 hours. The data is presented as a stacked bar chart, with the x-axis representing the hours of the day from 1 to 24, and the y-axis showing the average hourly generation in MW. The bars are segmented into different colors, each representing a distinct energy source: nuclear, bio, geothermal, solar, wind, hydro, natural gas, and other imports. The chart provides insights into the temporal variations in energy generation across different sources, highlighting the interplay between baseload and intermittent sources throughout the day.

Document	System of Record ¹						
	County Servers	Project View	OnBase	CGI Advantage Financial System	Purchasing Department		
Project plan/scope	W	T					
Project budgets	W	T	W	T			
Schedules/timeline (design)	W	T	W	T			
Schedules/timeline (construction)	W	T	W				
Executed contracts			W	T	W	T	
Purchase orders			W		W	T	
Solicitation advertisements			W	T	W	T	
Proposal submissions			W		W	T	
Selection committee evaluation documents			W	T	W	T	
Independent cost estimates		W	T	W		W	
Negotiation details		W			W		
Notice of award		T		W		W	
Notice to proceed		T		W		W	
Invoices/applications for payment ("AFP")		W	T	W	W	T	W
Change order requests		T		W			
Approved change orders		T	W	T	W		
Requests for Information (RFI)	W	T				W	T
Bid submissions				W		W	T
Shop drawings	W	T		T			
Photographs	W	T					
As-builts	W	T		T			
Operating manuals	W	T					
Maintenance schedules	W	T					
Warranties	W	T		T			
Daily diaries	N/A	T					
Weekly meeting minutes	W	T					
Monthly progress reports	W	T					
Allowance usage logs	W	T					
Punch lists	W	T					
Interim reports	W	T					

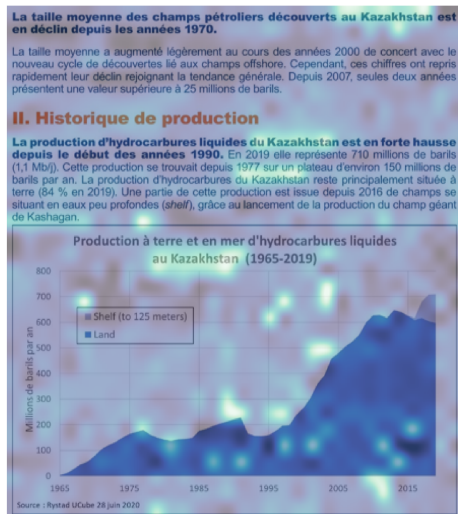
Figure 6: Example from the "Government Reports" test set.

Caption: The image shows a table titled "System of Record" which outlines the different types of documents or records maintained across various systems or departments within an organization related to project management and construction. The rows list documents like project plans, budgets, schedules, contracts, purchase orders, invoices, change requests, bid submissions, drawings, manuals, meeting minutes, and reports. The columns indicate the system or department responsible for maintaining each record, such as County Servers, Project View, OnBase, CGI Advantage Financial System, and Purchasing Department. The table uses "W" and "T" markers to denote which system or department serves as the primary source (writer) or storage location (trailer) for each type of document.

C More similarity maps

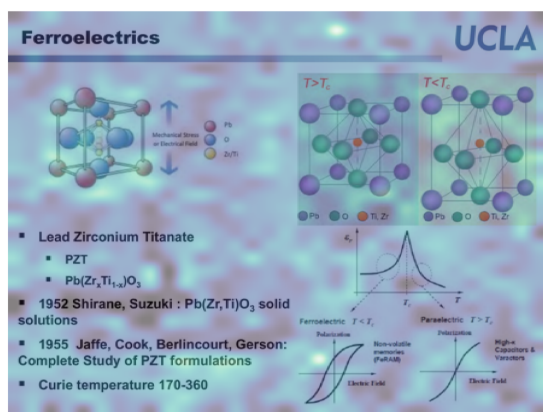
In Figure 7, ColPali assigns a high similarity to all patches with the word "Kazakhstan" when given the token <_Kazakhstan>. Moreover, our model seems to exhibit world knowledge capabilities as the patch around the word "Kashagan" - an offshore oil field in Kazakhstan - also shows a high similarity score. On the other hand, in Figure 8, we observe that ColPali is also capable of complex image understanding. Not only are the patches containing the word "formulations" highly similar to the query token _formula, but so is the upper-left molecule structure.

It is also interesting to highlight that both similarity maps showcase a few white patches with high similarity scores. This behavior might first seem surprising as the white patches should not carry a meaningful signal from the original images. We believe the vectors associated with these patches share a similar role with the ViT registers (Darcet et al., 2023), i.e. these patches were repurposed for internal computations and stored the global information from the whole image.



Query: "Quelle partie de la production pétrolière du Kazakhstan provient de champs en mer ?"

Figure 7: Similarity of the image patches w.r.t. the underlined token in the user query. This example is from the *Shift* test set.



Query: What is the chemical formula for the ferroelectric material Lead Zirconium Titanate (PZT)?

Figure 8: Similarity of the image patches w.r.t. the underlined token in the user query. This example is from the *Healthcare Industry* test set.

D Additional results

D.1 Other Metrics

	ArxivQ	DocQ	InfoQ	TabF	TATQ	Shift	AI	Energy	Gov.	Health.	Avg.
Unstructured <small>Text only</small>											
BM25	-	26.6	-	-	34.6	45.0	86.0	70.0	68.0	74.0	-
BGE-M3	-	22.8 _{↓3.8}	-	-	26.1 _{↓8.5}	51.0 _{↑6.0}	81.0 _{↓5.0}	72.0 _{↑2.0}	67.0 _{↓1.0}	77.0 _{↑3.0}	-
Unstructured <small>+ ocr</small>											
BM25	26.7	28.9	54.0	30.4	50.0	52.0	86.0	77.0	74.0	80.0	55.9
BGE-M3	28.1 _{↑1.4}	22.9 _{↓6.0}	53.8 _{↓0.2}	55.7 _{↑25.3}	38.6 _{↓11.4}	56.0 _{↑3.0}	82.0 _{↓4.0}	79.0 _{↑2.0}	76.0 _{↑2.0}	83.0 _{↑3.0}	57.5 _{↑1.6}
Unstructured <small>+ Captioning</small>											
BM25	35.5	30.2	61.5	24.3	49.0	47.0	79.0	76.0	75.0	81.0	55.9
BGE-M3	29.3 _{↓6.2}	26.0 _{↓4.2}	62.1 _{↑0.6}	58.6 _{↑34.3}	30.6 _{↓18.4}	55.0 _{↑8.0}	80.0 _{↑1.0}	78.0 _{↑2.0}	69.0 _{↓6.0}	83.0 _{↑2.0}	57.2 _{↑1.3}
Contrastive VLMs											
Jina-CLIP	19.4	7.3	26.7	12.5	1.6	2.0	11.0	13.0	15.0	17.0	12.6
Nomic-vision	10.4	6.7	22.1	9.6	1.6	0.0	9.0	9.0	7.0	13.0	8.8
SigLIP (Vanilla)	34.2	21.3	51.8	46.1	17.9	13.0	50.0	51.0	47.0	65.0	39.7
Ours											
(Copied) SigLIP (Vanilla)	34.2	21.3	51.8	46.1	17.9	13.0	50.0	51.0	47.0	65.0	39.7
BiSigLIP (+fine-tuning)	49.2 _{↑15.0}	23.8 _{↑2.5}	59.0 _{↑7.2}	52.1 _{↑6.0}	20.7 _{↑2.8}	16.0 _{↑3.0}	62.0 _{↑12.0}	61.0 _{↑10.0}	55.0 _{↑8.0}	72.0 _{↑7.0}	47.1 _{↑7.4}
BiPali (+LLM)	46.4 _{↓-2.8}	20.0 _{↓-3.8}	54.6 _{↓-4.4}	63.2 _{↑11.1}	20.4 _{↓-0.4}	34.0 _{↑18.0}	59.0 _{↓-3.0}	45.0 _{↓-16.0}	57.0 _{↑2.0}	56.0 _{↓-16.0}	45.6 _{↓-1.5}
<i>ColPali</i> (+Late Inter.)	72.4 _{↑26.0}	45.6 _{↑25.6}	74.6 _{↑20.0}	75.4 _{↑12.1}	53.1 _{↑32.7}	55.0 _{↑21.0}	93.0 _{↑34.0}	85.0 _{↑40.0}	85.0 _{↑28.0}	88.0 _{↑32.0}	72.7 _{↑27.1}

Table 4: **Comprehensive evaluation of baseline models and our proposed method on ViDoRe.** Results are presented using Recall@1 metrics. Text-only metrics are not computed for benchmarks with only visual elements.

D.2 Model Variants

	ArxivQ	DocQ	InfoQ	TabF	TATQ	Shift	AI	Energy	Gov.	Health.	Avg.
ColSigLIP (PaliGemma)	3.1	3.0	5.1	6.2	2.5	1.0	3.4	3.4	2.3	2.2	3.2
BiSigLIP (PaliGemma)	18.5	14.6	33.4	39.5	16.1	5.2	27.6	32.6	36.6	35.7	26.0
ColSigLIP (Original)	2.6	2.2	2.3	5.7	1.8	1.0	2.6	4.1	1.4	1.5	2.5
ColPali (No Mem. Tokens)	80.4	53.2	82.4	77.4	65.7	63.4	97.0	89.9	93.6	92.4	79.6
ColPali (Best)	79.1	54.4	81.8	83.9	65.8	73.2	96.2	91.0	92.7	94.4	81.3

Table 5: **Evaluation of some "negative results" and ablations on ViDoRe; ColPali for reference.** Results are presented using NDCG@5 metrics. Text-only metrics are not computed for benchmarks with only visual elements.

E ViDoRe examples

Energy

Query: What types of accounts or products allow investors to defer paying taxes?

Tax-efficient investing
Taxes have the potential to significantly affect your investment returns.

One way to help reach your financial goals is to be tax smart with your investments. You can affect your tax bill by paying attention to how and when you generate investment income, dividends, interest, and capital gains and losses. There are three strategies you can use to manage the potential impact on your federal income taxes:

- Defend:** Retirement savings accounts—including 401(k) and 403(b) plans, IRAs, health savings accounts (HSAs), and other tax-deferred products such as deferred annuities—all allow you to put off paying taxes.
- Manage:** Using asset location strategies, investing in lower turnover funds, understanding mutual fund distributions, and taking advantage of charitable gifts and capital loss deductions can all help you manage your tax burden.
- Reduce:** Consider tax-free investments, municipal bonds, HSAs, and college savings accounts to help reduce your taxes.

WAYS TO OPTIMIZE FEDERAL INCOME TAX RETURNS

Stocks: 10.5%
Stocks after taxes: 8.5%
Bonds: 6.5%
Bonds after taxes: 3.5%

Query: What is the projected peak electricity demand in California for the year 2030?

A Residential Customer Guide to Going Solar – R01-010

The savings shown in Tables 2 and 3 were calculated using typical energy usage data and PV output data for a 4.1 kW-sized system in Duke Energy Carolina territory. PV output data was obtained from NREL's PV Watts tool for the cities of Durham and Charlotte, and energy usage data was taken from NREL's dataset entitled "Commercial and Residential Hourly Load Profiles for all TMY3 Locations in the United States."

Table 2 shows estimated bill savings for each of the different performance-based payment choices paired with its available rate option. Savings for each option are based upon what the customer would otherwise be paying under the standard flat rate schedule with no PV system impact. The figures in Table 2 are averages of monthly savings calculated over the entire life of the PV system (25 years). As the savings are averaged over 25 years and assume a 2% annual increase in electricity costs, the bill amounts may appear higher than a typical customer's bill today. Savings will vary from month to month and over the years, but these estimates provide a useful comparison between the available options.

Table 3 displays estimated total savings for a PV system in Durham and Charlotte under each of the different billing options. In this example, net metering under flat rates and the new time-of-use pilot rate schedule are the most favorable options. As the results show, the rate option a customer chooses can have a significant impact on whether solar PV is a good investment for them.

Net Savings Over PV System Useful Life

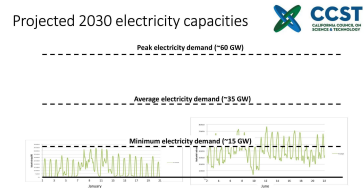
Rate/Billing Option	City	Low System Cost	Medium System Cost	High System Cost
Net Metering (Flat Rate)	Durham	\$10,618	\$8,788	\$6,983
	Charlotte	\$11,089	\$9,279	\$7,437
Net Metering (Time-of-Use Rate)	Durham	\$767	-\$1,049	-\$2,064
	Charlotte	\$444	-\$1,148	-\$1,983
Use Pilot Rate	Durham	\$9,053	\$7,737	\$5,922
	Charlotte	\$10,182	\$8,365	\$6,551
NC GreenPower Option A	Durham	\$510	-\$1,376	-\$1,111
	Charlotte	\$950	-\$116	-\$2,771
NC GreenPower Option B	Durham	\$800	-\$1,010	-\$1,035
	Charlotte	\$1,122	-\$694	-\$2,290

NOTE: Average savings values shown are not reported for PV systems in:

Table 3: Net Savings Over PV System Useful Life

NC GreenPower has the advantage of paying customers a premium for their RECs for the first five years, which can also help pay back the costs of the system quickly and reduce interest payments. However, it does not provide as much savings over the life of the system as the other options, since the NC GreenPower credits is limited to 5 years, and the amount each

Query: What is the estimated total savings for a PV system in Durham under the net metering (flat rate) billing option over the system's useful life of 25 years?



Artificial Intelligence

Query: What are some common outcome areas targeted by TAI for different age groups?

Technology Aided Instruction and Intervention (TAII)

Technology Aided Instruction and Intervention (TAII) are those in which technology is the central feature of an intervention. Given the opportunity to include technology in interventions, the evidence base is mixed to support its use to include technology that is specifically designed and evaluated to improve the learning and performance of students with different learning needs. A meta-analysis of 10 studies found that technology use in interventions had a small to moderate positive effect on student learning outcomes. The studies included in the meta-analysis were conducted in a variety of settings, including schools, after-school programs, and home-based learning environments. The studies included in the meta-analysis used a variety of outcome measures, including standardized test scores, self-reported learning outcomes, and teacher ratings of student learning. The meta-analysis found that technology use in interventions had a small to moderate positive effect on student learning outcomes, with the largest effects seen in studies that used technology to provide individualized instruction and feedback. The meta-analysis also found that technology use in interventions had a small to moderate positive effect on student learning outcomes, with the largest effects seen in studies that used technology to provide individualized instruction and feedback.

Outcome Area	Elementary School	High School	College
Communication	✓	✓	✓
Academic achievement	✓	✓	✓
Play	✓	✓	✓
Cognitive	✓	✓	✓
School readiness	✓	✓	✓
Language/Pre-academic	✓	✓	✓
Problem-solving	✓	✓	✓
Challenging/Complex	✓	✓	✓
Learning	✓	✓	✓
Motivation	✓	✓	✓
Mental health	✓	✓	✓
Self-administration	✓	✓	✓

Query: What did the robot monitor to determine when to activate or deactivate the blower motor and blinker?

2.4. Cotton Ball Harvest

To harvest the cotton bolls on the plant, a common reference coordinate was first established between the robot base with respect to the plant location, as shown in Figure 11. Both the relative position of the cotton bolls and the nozzle position were defined from this reference coordinate. Prior to harvesting, the average boll height and the offset for each row or plot to be compiled were measured to calibrate the nozzle position. The nozzle position was located based on how the nozzle of the cotton bolls were expected. The robot was then programmed to keep track of its relative position away from the plant as it navigates along the rows. The robot also monitored the user's position, which signals the activation or deactivation of the blower motor and blinker to start or end the harvesting.

2.5. Study Site

An 82 x 142 sq m 20-row karyo sand field of cotton (Deltapine 1598 B2DF) was established with 10 rows spacing and 80 rows rows plant spacing at the Edin Research and Education Center in Black Hill, NC (33°55'N, 81°27'W). Seeding was done in early May and harvesting in the last week of November. Regular crop management practices were applied during the growing season. Laboratory and field tests were conducted to configure and evaluate the navigation and harvesting system's performance before they were integrated.

2.6. Global Positioning System (GPS) and Laser Scanner Setup and Mapping

Key components of the navigation and harvesting system were first tested to determine if it was suitable for the study's objectives and requirements. Off-board GPS, laser scanner, and other important components (i.e., blower motor, base unit, nozzle type, and tool) were all subjected to test trials. Not only the GPS and laser scanner will be presented, as these were the critical factors in autonomous navigation. For GPS, outdoor survey measurements were conducted to determine the longitude and latitude readings' accuracy per waypoint. Before sampling sites chosen for the study, the accuracy of the GPS was tested in a simulated environment. In the test, results of 2-m accuracy for the user were used as a simulated cotton stem. The bolls were fixed by using the left and right edges. Due to the length of the bolls, the laser scanner cannot be moved to the lower frame. For mapping, testing took place in both indoor and outdoor environments. For the indoor environment test, a 14.6-ft platform was used as the base and a navigation laboratory and the whole building, which the laboratory is located. The outdoor mapping test was conducted on the field with live rows.

2.7. Performance Evaluation

The performance of the robot in cotton harvesting was first conducted in the laboratory in terms of how effectively the harvester sectioned the cotton bolls and how close they should

Query: What is the key approach used in the PDP architecture?

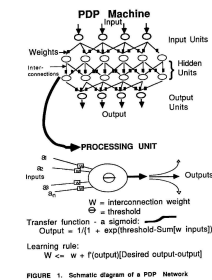


FIGURE 1. Schematic diagram of a PDP Network

A key approach in the PDP architecture is the use of an adaptive filter. The adaptive filter can accept a real-world analog input and compare it to a stored pattern. The stored pattern represents the desired input level which can then be modified as necessary so that eco-free signals can produce the correct results. A more abstract argument driving the design of the PDP network is machine efficiency, that is, the optimal utilization of the Neumann architecture most of the computer's capacity if the memory is used as active as possible. In the more familiar structure of a modern computer (the von Neumann architecture) most of the computer's capacity is used as passive storage. This is very useful from a pure resource management standpoint. The main of the time, this is very useful from a pure resource management standpoint. The main of the time, this is very useful from a pure resource management standpoint. The main of the time, this is very useful from a pure resource management standpoint.

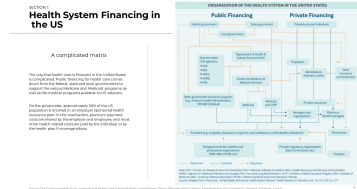
Healthcare Industry

Query: What is the chemical formula for the ferroelectric material Lead Zirconium Titanate (PZT)?

Ferroelectrics

- Lead Zirconium Titanate
 - PZT
 - Pb(Zr,Ti)_{1-x}O₃
- 1952 Shirane, Suzuki : Pb(Zr,Ti)O₃ solid solutions
- 1955 Jaffe, Cook, Berlincourt, Gerson: Complete Study of PZT formulations
- Curie temperature 170-360

Query: What government entities are involved in public financing for healthcare in the US?



Query: What does the AVPU scale stand for in assessing the level of consciousness of a seriously ill child?

Paediatric emergencies

Assessment of the seriously ill child

AVPU
Alert
Responsive to voice
Responsive to pain
Unresponsive

Capillary refill time

Other emergency interventions

Box 6.3 AVPU rapid assessment of level of consciousness

Basic life support

Advanced life support

The seriously injured child

Government Reports

Query: What are some mandates for the EPA under the Pollution Prevention Act?

APPENDIX II – CURRENT POLLUTION PREVENTION MANDATES IN FEDERAL STATUTES

Federal Act	Section	Pollution Prevention Mandate
Pollution Prevention Act (PPA)	13101	EPA mandated to develop and implement a strategy to promote source reduction.
	13104	EPA as administrator is given the authority to provide grants to the States to promote source reduction by businesses.
	13105	EPA mandated to establish a database that contains information on source reduction.
Clean Air Act (CAA)	13106	Owners and operators of businesses that are required to file a toxic chemical release form must include a toxic reduction and recycling report.
	7402	Encourages cooperation amongst the federal departments, states, and local governments for prevention and control of air pollution.
	7403	EPA mandated to establish a national research and development program for prevention and air pollution control.
	7405	Also, EPA must facilitate coordination amongst air pollution prevention and control agencies.
	7405	EPA can make grants to air pollution prevention and control agencies.
	7412	Facilities that reduce their emission of toxics into the air by 90-95% can qualify for permit waivers.
	7414 and 7415	EPA may establish record keeping, inspection, and monitoring for all facilities that emit pollutants.
Subchapter I, Part C, Sec. 7470-7479		Prevention of significant deterioration of air quality establishment of a plan that includes emission limitations to protect public welfare and the environment.
		General emissions standards

Query: What is the strategy of KPMG Hazem Hassan?

Who we are?

Our business: KPMG Hazem Hassan is a professional services firm that delivers Audit, Tax and Advisory services. We operate out of two offices across Egypt without an average of 100 employees and operations in the period 13 December 2020 (2019: 100).

Our audit services in Egypt are delivered through KPMG Hazem Hassan Public Accountants and Consultants. Full details of the services offered by KPMG Hazem Hassan can be found at our website: <https://www.kpmg.com/egypt/About-us/Our-business>

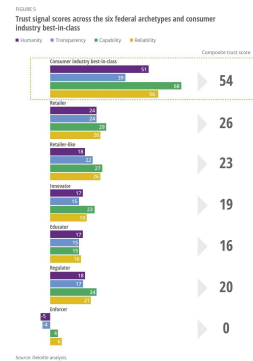
Our strategy: Our strategy is set by the KPMG Egypt management Board and as well as our supporting our reputation as the best firm to work with by employing our people and company's activities to full potential.

Employer of choice | **Industry knowledge**

Our people | **Our clients**

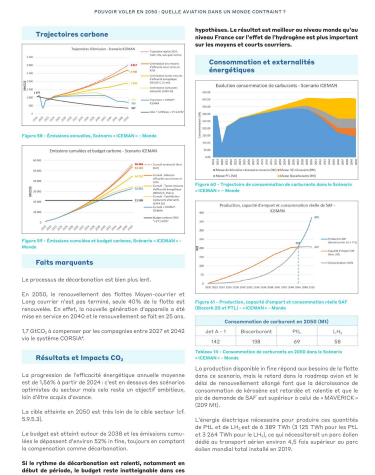
Multidisciplinary capabilities | **Global consistency**

Query: What is the trust signal score for the consumer industry best-in-class archetype?



Shift

Query: Selon le graphique, quelle est la capacité d'import et la consommation réelle de carburants SAF (bio-carburants durables pour l'aviation) prévues en 2050 ?



Query: Quelle partie de la production pétrolière du Kazakhstan provient de champs en mer ?



Query: Quels sont les pays ayant la plus grande part des découvertes cumulées de pétrole brut en 2020 (en milliers de barils, hors découvertes cumulées) ?

B. L'exemple de la Feuille de route de décarbonation, de Health Care Without Harm et ARUP

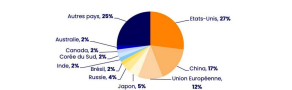
En avril 2021, Health Care Without Harm et ARUP ont publié une Feuille de route de décarbonation, basée sur le rapport "Green Paper Check" d'avril 2019, dans lequel ils ont défini les principes de décarbonation du secteur de la santé.

Pour cela, ils ont défini le périmètre du secteur de la santé et ils ont utilisé la World Input Output Database qui fournit un modèle complet du commerce mondial pour 59 secteurs différents et ce, pour 68 nations différentes¹¹. Ce modèle leur permettrait alors de modifier les flux physiques (de marchandises, d'énergie, etc.) existant entre différents pays dans le cadre du secteur de la santé et ainsi, d'estimer les émissions de GES associées.

Dans ce rapport de Health Care Without Harm, l'empreinte carbone du secteur de la santé a été évaluée à 4,4 % des émissions mondiales. Parmi ce secteur, il est le plus grand émetteur de la planète. Le rapport identifie également les principales sources d'émissions, ce qui constitue une première étape dans l'établissement d'une feuille de route pour la décarbonation du secteur de la santé. En outre, il montre que les émissions industrielles (scope 3) représentent la plus grande part avec 71 % des émissions (Figure 11).



Ce rapport montre également que les pays dont l'empreinte carbone est la plus forte sont aussi les pays dont le secteur de la santé émet le plus de GES. Ainsi, les États-Unis, la Chine et l'Union européenne sont les trois principaux contributeurs à l'empreinte climatique du secteur de la santé. Or, plus de 50 % des principales émissions de carbone du secteur de la santé représentent 75 % des émissions mondiales totales du secteur (Figure 12).



En outre, il évalue l'empreinte carbone du système de santé français à 20 MCO, soit 4,6 % des émissions du pays (hors émissions de réchauffement climatique). La feuille de route pour